*Journal of Organometallic Chemistry, 482* (1994) 99–109

# 1,3-Dipolar cycloaddition to the C=X–M fragment

# 13. Regioselectivity in the reactions of mononuclear iminoketone complexes $Fe(CO)_3(^tBu\text{-}N=C(H)-C(R)=O)$ (R = Ph, Me) with the asymmetric alkyne methyl propynoate

Maarten van Wijnkoop, Ron Siebenlist, Jan M. Ernsting, Paul P.M. de Lange
and Hans-Werner Frühauf

*Laboratorium voor Anorganische Chemie, J.H. van 't Hoff Instituut, Universiteit van Amsterdam, Nieuwe Achtergracht 166, 1018 WV Amsterdam (Netherlands)*

Ernst Horn and Anthony L. Spek

*Bijvoet Center for Biomolecular Research, Vakgroep Kristal- en Structuurchemie, Universiteit Utrecht, Padualaan 8, 3584 CH Utrecht (Netherlands)*

(Received January 14, 1994)

## Abstract

The reaction of complexes $Fe(CO)_3(^tBu\text{-}N=C(H)-C(R)=O)$ (**6a**: R = Ph, **6b**: R = Me) with one equivalent of methyl propynoate (MP) under an atmosphere of CO, at −30°C (R = Ph) or −50°C (R = Me) results in formation of the $Fe(CO)_3$(butenolide) complexes (**9a,b**), which have been characterized spectroscopically (IR, $^1H$, $^{13}C$ NMR) and by elemental analysis. The spectroscopic properties indicate that one of the possible regio-isomers is exclusively formed. INEPT and 2D heteronuclear correlation NMR techniques show that in the regio-isomer obtained the former ketone carbon atom is C–C bonded to the carbon atom that in the alkyne bore the electron-withdrawing ester group. When the complexes $Fe(CO)_3(^tBu\text{-}N=C(H)-C(R)=O)$ (**6a,b**) are treated with two equivalents of MP at −30°C in the absence of CO, the tricyclic complexes **12a,b** are formed in moderate yield. The molecular structure of complex **12b** has been determined by a single-crystal X-ray diffraction study. It contains three five-membered rings, with the two fused metallacycles sharing three common carbon atoms with the third, a γ-lactone ring, thus forming the tricyclic moiety. The coordination geometry around the central iron atom is distorted octahedral, with the dianionic tridentate ligand occupying three facial positions. The fact that complexes **12** can also be obtained in high yield by irradiation of the corresponding $Fe(CO)_3$(butenolide) (**9**) in the presence of an excess of MP strongly supports the proposed reaction mechanism in which the second alkyne is initially π-coordinated and subsequently coupled with the π-coordinated double bond of the butenolide heterocycle.

*Key words:* Iron; Carbonyl; Alkynes; Cycloaddition; Crystal structure

## 1. Introduction

In the first papers in this series we reported on the reactions of (1,4-diaza-1,3-butadiene) tricarbonyliron complexes (**1**) with dimethyl acetylenedicarboxylate (DMADC[1*]) which give (1,5-dihydropyrrol-2-one)-$Fe(CO)_3$ complexes (**5**) (cf Scheme 1; X = N) [2a,b]. Additional research on the influences of the coligands, the metal and the substitution pattern of both the DAB-ligand and the activated alkyne provided us with

---

Correspondence to: Dr. H.-W. Frühauf.

[*] Reference numbers with asterisk indicate a note in the list of references.

0022-328X/94/$7.00
*SSDI* 0022-328X(94)24606-J

more detailed information about the influences on the product formation and the mechanism of this type of reaction. The initial step in these reactions can be described as an oxidative 1,3-dipolar cycloaddition of the activated alkyne to the M–N=C fragment, resulting in the formation of the bicyclo[2.2.1] intermediate **2**. This proposal is firmly supported by the isolation and characterization of a N-protonated ruthenabicyclo [2.2.1] complex [2g] and by the formation of the M(CO)$_2$L(THPP) complexes (**4**) in the presence of an excess of the alkyne [2f–h].

In order to extend the scope of this type of reaction in synthesis we decided to investigate the behaviour of the closely related $\sigma$-O, $\sigma$-N chelate Fe(CO)$_3$(1-aza-4-oxo-butadiene) complexes with DMADC and found that they exhibit similar reactivity (cf. Scheme 1, X = O) [2i]. The exclusive formation of the Fe(CO)$_3$(butenolide) complexes **5** indicates that in the latter reactions the initial 1,3-dipolar cycloaddition of the activated alkyne proceeds with complete chemoselectivity to the Fe–O=C fragment. Apparently the coordinated C=O fragment is, as a result of both steric and electronic influences, more reactive towards electron deficient dipolarophiles than is the coordinated C=N fragment.

This increase in reactivity prompted us to investigate whether the Fe(CO)$_3$(1-aza-4-oxo-butadiene) complexes would also react with less electron deficient alkynes. The obvious choice was methyl propynoate (MP) as alkyne, because MP has been shown to react very slowly and only at elevated temperatures with Fe(CO)$_3$($^i$Pr-DAB) [2d], and it would also allow us to obtain information about the regioselectivity in the initial reaction step. In the case of Fe(CO)$_3$($^i$Pr-DAB) only one regio-isomer (Scheme 1, complex **5**, R′ = H) is obtained.

The present report focuses on the products formed in the reactions of Fe(CO)$_3$($^t$Bu-N=C–(R)=O) (R = Ph, Me) with MP. Which product is formed depends strongly on the additional ligand offered; in the presence of CO one of the possible regioisomeric Fe(CO)$_3$(butenolide) complexes is exclusively obtained, whereas in the presence of an excess of MP a second regioselective C–C coupling occurs to give a tricyclic iron(II) complex. The X-ray crystal structure of one of these tricyclic complexes (R = Me) is presented.

## 2. Experimental section

### 2.1. Materials and apparatus

$^1$H and $^{13}$C NMR spectra were recorded on Bruker AC 100 or AMX 300 spectrometers. The IR spectra were recorded on a Perkin-Elmer 283 IR spectrophotometer. The preparative scale irradiations were carried out using a Philips HPK 125 W high pressure mercury lamp equipped with a Pyrex glass filter ($\lambda \geq$ 280 nm). Elemental analyses were carried out by the Elemental Analysis section of the Institute for Applied Chemistry, TNO, Zeist, The Netherlands, and Dornis

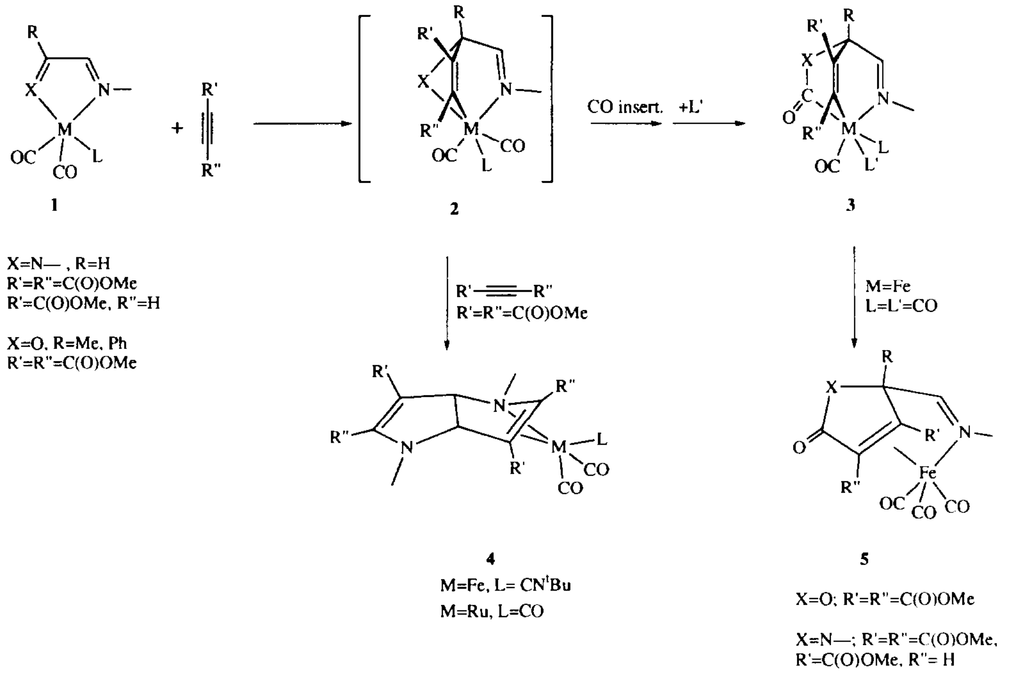

Scheme 1.

u. Kolbe, Microanalytisches Laboratorium, Mülheim a.d. Ruhr, Germany.

The solvents were carefully dried and distilled under nitrogen prior to use. All preparations were carried out under dry nitrogen by conventional Schlenk techniques. Silica gel used for column chromatography (Kieselgel 60, 70-230 mesh, E. Merck, Darmstadt, Germany) was dried and activated prior to use. Methyl propynoate (MP) was used as purchased from Aldrich. The $\alpha$-iminoketones ($^t$Bu-N=C(H)–C(R)=O) (R = Ph, Me) [3] and Fe(CO)$_3$($^t$Bu-N=C(H)–C(R)=O) (**6a**: R = Ph; **6b**: R = Me) complexes [2i] were prepared by published procedures. It is advisable to use freshly prepared pentane solutions of complexes **6** because removal of the solvent and storage of these complexes gives rise to partial decomposition and subsequent reactions, that result in formation of dinuclear species.

#### 2.1.1. *Synthesis of Fe(CO)$_3$–N($^t$Bu)=C(H)–C(Ph)-C(CO$_2$CH$_3$)=C(H)C(O)O (9a)*

A freshly prepared solution of 5.7 mmol Fe(CO)$_3$-($^t$Bu-N=C(H)–C(Ph)=O) (**6a**) in 80 mL of pentane (*vide supra*) was cooled to −30°C under an atmosphere of CO (1.2 bar) and a solution of 530 $\mu$l (5.9 mmol) of MP in 50 ml of pentane/diethyl ether (4:1) was added dropwise during *ca.* 45 min. The mixture was stirred for an additional one hour at −30°C, during which the initially deep-purple solution turned pale purple and the yellow-brown crude product separated out. The supernatant liquid was decanted and the residue washed twice with 30 ml of pentane/diethyl ether (3:1) at −30°C and dried *in vacuo*. The crude product was then redissolved in 2–4 ml of CH$_2$Cl$_2$ and purified by column chromatography on silica. Elution with pentane/diethyl ether (3:2) afforded a yellow fraction, which was evaporated to dryness to yield 1.81 g (4.1 mmol, 72%) of the bright yellow complex **9a**. Recrystallization of **9a** from diethyl ether at −20°C gave yellow needles.

#### 2.1.2. *Synthesis of Fe(CO)$_3$–N($^t$Bu)=C(H)–C(Me)-C(CO$_2$CH$_3$)=C(H)C(O)O (9b)*

A freshly prepared solution of 7.7 mmol Fe(CO)$_3$-($^t$Bu-N=C(H)–C(Me)=O) (**6b**) in 80 ml of pentane (*vide supra*) was cooled to −50°C under an atmosphere of CO (1.2 bar) and a solution of 715 $\mu$l (8.0 mmol) of MP in 50 ml of pentane/diethyl ether (4:1) was added dropwise during *ca.* 45 min. During the reaction the initially deep purple solution became paler and the dark brown crude product separated out. The supernatant ligand was decanted and the residue washed twice with 30 ml of pentane/diethyl ether (3:1) at −30°C and dried *in vacuo*. It was then redissolved in 3–5 ml of CH$_2$Cl$_2$ and purified by column chromatography on silica. Elution with diethyl ether/CH$_2$Cl$_2$ (10:1) afforded a yellow-brown fraction, which was evaporated to dryness. The yellow-brown residue was washed twice with 10 ml of diethyl ether/pentane (2:1) and dried *in vacuo* to yield 2.2 g (5.8 mmol, 75%) of bright yellow **9b**. Yellow needles were obtained by slow addition of THF to a suspension of 300 mg of the product in 2.5 ml of diethyl ether until the product was completely dissolved, and keeping the solution at −30°C for several days.

#### 2.1.3. *Synthesis of the tricyclic complex 12a*

A freshly prepared solution of 5.2 mmol Fe(CO)$_3$-($^t$Bu-N=C(H)–C(Ph)=O) (**6a**) in 80 ml of pentane (*vide supra*) was cooled to −30°C and a solution of 950 $\mu$l (10.7 mmol) of MP in 40 ml of pentane/diethyl ether (4:1) was added dropwise during *ca.* 45 min. and the solution was stirred for an additional hour. During the reaction the initially deep purple solution became paler and the dark brown crude product separated out. The supernatant liquid was decanted and the residue washed twice with 30 ml of pentane/diethyl ether (3:1) at −30°C and dried *in vacuo*. It was then redissolved in 10 ml of CH$_2$Cl$_2$ and purified by column chromatography on silica. Elution with diethyl ether/CH$_2$Cl$_2$ (9:1) afforded a dark brown fraction, which was evaporated to dryness. The residue still contained impurities, and so was suspended in 20 ml of diethyl ether and again chromatographed on silica. Elution with diethyl ether afforded a reddish-brown fraction, which was evaporated to dryness. The residue was washed once with 10 ml of pentane/diethyl ether (4:1) and four times with 10 ml of pentane and then dried in vacuo to yield 1.9 g (3.6 mmol, 70%) of pure, beige-coloured **12a**. Off-white crystals were obtained by recrystallization from diethyl ether/pentane (5:1) at −20°C.

#### 2.1.4. *Synthesis of the tricyclic complex 12b*

The complex was prepared by the procedure used for **12a**, but starting from 8.1 mmol Fe(CO)$_3$($^t$Bu-N=C(H)–C(Me)=O) (**6b**) and 1.5 ml (16.6 mmol) of MP at −50°C. The eluents used for the subsequent purifications by chromatography on silica gel were slightly different; in the first passage through the column diethyl ether/CH$_2$Cl$_2$ (1:5) was used, and in the second diethyl ether/CH$_2$Cl$_2$ (20:1) was used. Complex **12b** was obtained as beige powder in a yield of 2.25 g (4.9 mmol, 60%) Off-white crystals suitable for X-ray diffraction were obtained by slow addition of THF to a suspension of 300 mg of the product in 2.5 ml of diethyl ether until the product had completely dissolved, and keeping the solution at −30°C for several days.

### *2.2. Photochemical preparation of complex 12 from complexes 9*

#### *2.2.1. Complex **12a***

A solution of 35 μl (0.39 mmol) of MP and 110 mg (0.25 mmol) of complex **9a** in 40 ml of diethyl ether was irradiated at room temperature. After *ca.* 30 min the colour of the solution had changed from yellow to light brown and the IR spectrum revealed that all the starting complex had disappeared. The solution was evaporated to dryness and the brown-grey crude product was washed three times with 20 ml of pentane/diethyl ether (3 : 1) to remove the excess of MP and then dried in vacuo, yielding 110 mg (0.21 mmol, 85%) of gray **12a**.

#### *2.2.2. Complex **12b***

The complex was prepared analogously to complex **12a** but starting from a solution of 46 μl (0.51 mmol) of MP and 110 mg (0.29 mmol) of complex **9b** in 20 ml of THF, and yielding 120 mg (0.26 mmol, 90%) of beige-gray **12b**.

### *2.3. Crystal structure determination and refinement of **12b***

The crystallographic data and numerical details for the complex **12b** are listed in Table 1. An opaque white crystal was mounted on top of a glass fibre and transferred to an Enraf-Nonius CAD4 diffractometer for data collection at 100 K. Lattice parameters were derived from the SET4 setting angles of 25 reflections with $13 < \theta < 20°$. The reflection data were corrected for Lp, but not for absorption. The structure was solved with the PATT option of SHELXS-86 [4] and refined by full-matrix least squares on F (SHELX-76) [5]. Hydrogen atoms were included at calculated positions (C–H = 0.97 Å) and refined riding on their carrier atoms with one common isotropic thermal parameter. Convergence was reached at $R = 0.032$, $R_w = 0.048$.

Neutral atom scattering factors were taken from Cromer and Mann (1968) [6] and corrected for anomalous dispersion [7]. Geometrical calculations and the thermal motion ellipsoid plot were performed with the program PLATON [8]. All calculations were carried out on a Micro VAX-II cluster. A list of hydrogen atom

TABLE 1. Crystallographic data and details of data collection and refinement for **12b**

| | |
|---|---|
| *(a) Crystal data* | |
| Formula | $C_{19}H_{21}NO_9Fe$ |
| Mw | 463.22 |
| Crystal system | triclinic |
| Space group | $P\bar{1}$ (Nr. 2) |
| $a$, $b$, $c$ (Å) | 8.569(1), 8.754(1), 14.782(3) |
| $\alpha$, $\beta$, $\gamma$ (°) | 88.84(1), 80.41(1), 68.38(1) |
| $V$(Å$^3$), $Z$ | 1015.4(3), 2 |
| $d_{(calc)}$ (g cm$^{-3}$) | 1.515 |
| $F$(000) | 480 |
| $\mu$ (cm$^{-1}$) | 7.9 |
| Crystal size (mm$^3$) | 0.30 × 0.40 × 0.60 |
| *(b) Data collection* | |
| Temperature (K) | 100 |
| $\theta_{min}$, $\theta_{max}$ | 1.40, 27.50 |
| Radiation | Mo $K_\alpha$ (Zr-filtered), 0.71073 Å |
| Scan type | $\omega/2\theta$ |
| $\Delta\omega$ (°) | 0.70 + 0.35 tan$\theta$ |
| Hor. and vert. aperture (mm) | 3.50, 5.00 |
| Reference reflections | 03 −1, −1 0 −4, −3 −3 0 |
| Data set | $h$ −11: 0; $k$ −11: 10, l −19: 18 |
| Total data | 4971 |
| Total unique data | 4657 |
| Obsd. data ($I > 2.5\sigma(I)$) | 4075 |
| *(c) Refinement* | |
| No. of refined parameters | 273 |
| Weighting scheme | $w = 1.1343/[\sigma^2(F) + 0.000841\ F^2]$ |
| Final $R$, $R_w$, $S$ | 0.0324, 0.0477, 0.67 |
| $(\Delta/\sigma)_{max}$, $(\Delta/\sigma)_{av}$ | 0.15, 0.02 |
| Res. density (min, max) e Å$^3$ | −0.52, 0.76 |

coordinates and a table of anisotropic thermal parameters has been deposited at the Cambridge Crystallographic Data Centre.

## 3. Results and discussion

### 3.1. Reactions with MP under CO

When the complexes Fe(CO)$_3$($^t$Bu-N=C(H)-C(R)=O) (**6a**: R = Ph; **6b**: R = Me) are reacted at $-30^\circ$C and $-50^\circ$C respectively, with one equivalent of MP under an atmosphere of CO (1.2 bar) the Fe(CO)$_3$ (butenolide) complexes **9** are obtained in good yields (cf. Scheme 2). Complexes **9** are airstable and soluble in common organic solvents (except in alkanes). They have been characterized by IR, $^1$H and $^{13}$C NMR spectroscopy and elemental analysis. The reaction of complex **6a** with MP is somewhat slower, which can probably be attributed to the electron withdrawing properties of the phenyl substituent that lowers the reactivity of the Fe–O=C 1,3-dipole (*vide infra*). A similar behaviour has been observed in the reactions of complexes **6** with DMADC [2i]. The finding that complexes **6** readily react with MP at low temperatures supports the presumption that the Fe–O=C fragment is more reactive towards electron deficient alkynes than the Fe–N=C fragment in Fe(CO)$_3$(R-DAB), which has been shown only to react with MP under more forcing conditions (9 days at 40°C to obtain complete conversion) [2d]. It is evident from the $^1$H and $^{13}$C NMR data that exclusively one of the possible regio-isomeric Fe(CO)$_3$(butenolide) complexes is formed (see Fig. 1). With the use of INEPT and heteronuclear 2D NMR techniques this isomer was identified as regio-isomer A, i.e. with the one in which the carbon of the carbonyl group has become bonded to the alkyne carbon atom bearing the ester group. An explanation of the observed regioselectivity is presented below in the section on complex formation.

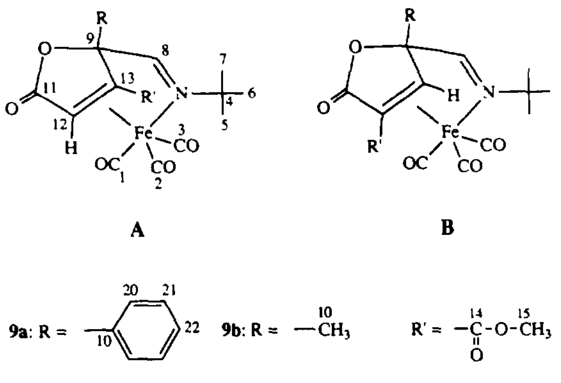

Fig. 1. Possible regio-isomers of complexes **9**, with the atom labeling.

### 3.2. Reactions with an excess of MP

If the reactions of complexes **6** with MP are carried out in the absence of CO a significant amount of a second product can be isolated. According to its spectroscopic properties this contains two equivalents of MP. In order to increase the yield of this product we performed the reactions of complexes **6** with two equivalents of MP in the absence of other additional ligands and obtained exclusively the tricyclic complexes **12** in moderate yields (Scheme 2). The tridentate hetero-

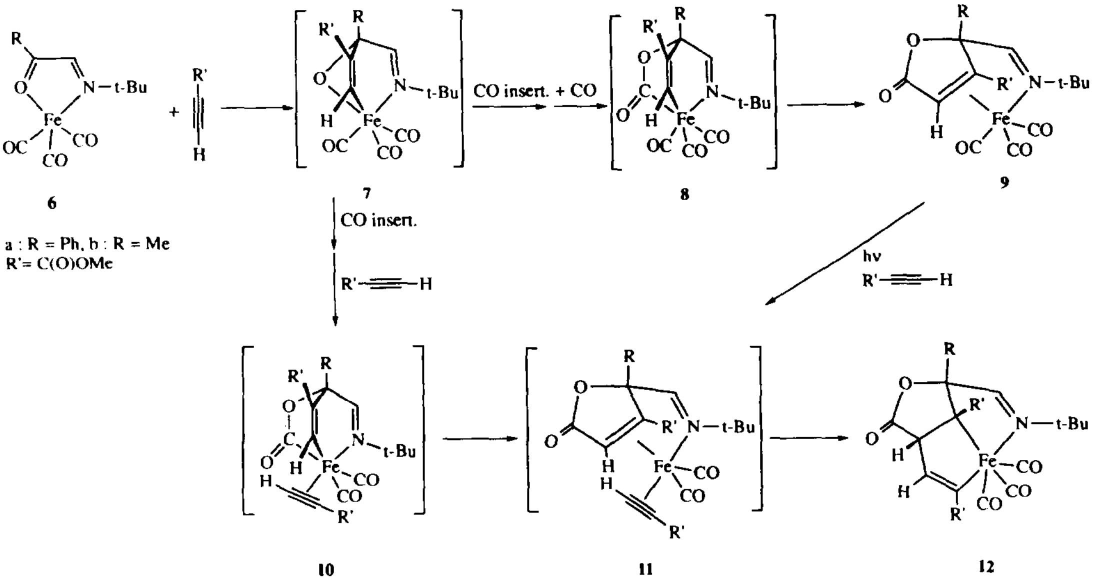

Scheme 2.

cyclic ligand in **12** is most likely formed *via* C–C coupling of the $\pi$-coordinated butenolide C=C bond with the initially $\pi$-coordinated MP moiety. The presence of one set of resonances in the $^{1}H$ and $^{13}C$ NMR spectra of **12** and the mutual coupling constant for the resonances assigned to the former MP and butenolide protons ($^{3}J = 3.3$ Hz) indicate that only one of the four possible linkage isomers is formed. This was confirmed by the crystal structure of complex **12b** (*vide infra*). Complexes **12** can also be prepared in almost quantitative yield by irradiation of the corresponding complexes **9** in the presence of excess MP at room temperature, which strongly supports the proposed reaction mechanism (see complex formation). The high yields obtained in the latter reactions indicates that practically all the CO that is initially displaced by the second MP moiety stays in solution, and is subsequently taken up to occupy the vacant coordination site in the 16-electron Fe(II) species that is formed after the C–C coupling. The latter reactions provide an outstanding example of the chemo- and regio-selectivities encountered in metal-directed organic synthesis. Of the eight possible isomers (sixteen if the possible cycloaddition across the Fe–N=C moiety is included) only one is formed.

### 3.3. *Molecular structure of the tricyclic complex 12b*

An ORTEP drawing with the numbering scheme of **12b** is shown in Fig. 2, the bond distances and angles and fractional coordinates are given in Tables 2 and 3, respectively.

TABLE 2. Bond distances (Å) and angles (°) of the non-hydrogen atoms in **12b** (e.s.d.'s in parentheses)

| | | | | | |
|---|---|---|---|---|---|
| Fe–N | 2.0499(16) | O(5)–C(11) | 1.199(2) | C(4)–C(7) | 1.530(3) |
| Fe–C(1) | 1.8390(18) | O(6)–C(14) | 1.207(2) | C(8)–C(9) | 1.499(3) |
| Fe–C(2) | 1.7710(18) | O(7)–C(14) | 1.342(2) | C(9)–C(10) | 1.523(3) |
| Fe–C(3) | 1.8264(18) | O(7)–C(15) | 1.450(3) | C(9)–C(13) | 1.542(2) |
| Fe–C(13) | 2.1129(17) | O(8)–C(18) | 1.210(2) | C(11)–C(12) | 1.514(2) |
| Fe–C(17) | 2.0045(18) | O(9)–C(18) | 1.350(2) | C(12)–C(13) | 1.543(2) |
| O(1)–C(1) | 1.130(2) | O(9)–C(19) | 1.445(2) | C(12)–C(16) | 1.493(2) |
| O(2)–C(2) | 1.143(2) | N–C(4) | 1.514(2) | C(13)–C(14) | 1.508(3) |
| O(3)–C(3) | 1.138(2) | N–C(8) | 1.272(2) | C(16)–C(17) | 1.341(2) |
| O(4)–C(9) | 1.482(2) | C(4)–C(5) | 1.537(2) | C(17)–C(18) | 1.490(2) |
| O(4)–C(11) | 1.354(2) | C(4)–C(6) | 1.526(2) | | |

| | | | |
|---|---|---|---|
| N–Fe–C(1) | 89.95(7) | N–C(8)–C(9) | 121.09(16) |
| N–Fe–C(2) | 169.61(7) | O(4)–C(9)–C(8) | 104.12(14) |
| N–Fe–C(3) | 99.15(7) | O(4)–C(9)–C(10) | 105.60(13) |
| N–Fe–C(13) | 82.55(6) | O(4)–C(9)–C(13) | 105.80(13) |
| N–Fe–C(17) | 87.55(7) | C(8)–C(9)–C(10) | 108.83(14) |
| C(1)–Fe–C(2) | 97.06(8) | C(8)–C(9)–C(13) | 110.36(14) |
| C(1)–Fe–C(3) | 89.93(8) | C(10)–C(9)–C(13) | 120.73(17) |
| C(1)–Fe–C(13) | 91.87(7) | O(4)–C(11)–O(5) | 121.26(16) |
| C(1)–Fe–C(17) | 174.33(7) | O(4)–C(11)–C(12) | 110.43(14) |
| C(2)–Fe–C(3) | 88.56(8) | O(5)–C(11)–C(12) | 128.31(16) |
| C(2)–Fe–C(13) | 89.54(7) | C(11)–C(12)–C(13) | 105.55(13) |
| C(2)–Fe–C(17) | 84.77(8) | C(11)–C(12)–C(16) | 112.56(15) |
| C(3)–Fe–C(13) | 177.53(7) | C(13)–C(12)–C(16) | 111.61(13) |
| C(3)–Fe–C(17) | 95.49(7) | Fe–C(13)–C(9) | 106.19(11) |
| C(13)–Fe–C(17) | 82.77(7) | Fe–C(13)–C(12) | 109.62(11) |
| C(9)–O(4)–C(11) | 110.42(13) | Fe–C(13)–C(14) | 109.02(11) |
| C(14)–O(7)–C(15) | 115.57(16) | C(9)–C(13)–C(12) | 102.91(14) |
| C(18)–O(9)–C(19) | 115.12(14) | C(9)–C(13)–C(14) | 114.89(14) |
| Fe–N–C(4) | 128.01(11) | C(12)–C(13)–C(14) | 113.79(14) |
| Fe–N–C(8) | 114.09(13) | O(6)–C(14)–O(7) | 122.31(17) |
| C(4)–N–C(8) | 117.83(15) | O(6)–C(14)–C(13) | 125.59(16) |
| Fe–C(1)–O(1) | 175.54(16) | O(7)–C(14)–C(13) | 112.00(15) |
| Fe–C(2)–O(2) | 177.81(16) | C(12)–C(16)–C(17) | 118.72(16) |
| Fe–C(3)–O(3) | 171.40(17) | Fe–C(17)–C(16) | 116.85(13) |
| N–C(4)–C(5) | 106.72(14) | Fe–C(17)–C(18) | 124.65(12) |
| N–C(4)–C(6) | 109.12(13) | C(16)–C(17)–C(18) | 118.43(15) |
| N–C(4)–C(7) | 112.58(14) | O(8)–C(18)–O(9) | 122.53(16) |
| C(5)–C(4)–C(6) | 111.57(14) | O(8)–C(18)–O(17) | 124.69(17) |
| C(5)–C(4)–C(7) | 108.53(14) | O(9)–C(18)–O(17) | 112.77(14) |
| C(6)–C(4)–C(7) | 108.35(15) | | |

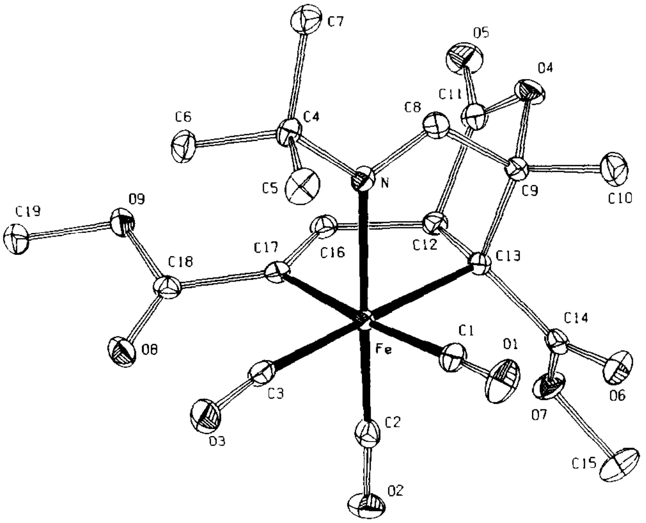

Fig. 2. Thermal motion ellipsoid plot (at the 50% probability level) for Complex **12b**.

The central iron atom in complex **12b** has a slightly distorted octahedral coordination geometry and is bonded to the newly formed tridentate dianionic ligand. The intact imine substituent (C(8)–N = 1.272(2) Å) at the 2-position of the five-membered lactone ring is coordinated to iron via the nitrogen atom by a normal $\sigma$-donative bond (Fe–N = 2.0499(16) Å), while the alkene substituent attached to the 4-position of the lactone is covalently bound to the iron atom *via* C(17). The Fe–C(17) distance of 2.0045(18) Å is within the range generally observed for this type of Fe–$C_{sp^2}$ bond [9b,10]. The former alkyne carbon atom C(13) at the 3-position of the lactone ring is also covalently bound to iron, thus completing the tricyclic structure of the complex. The Fe–C(13) bond distance of 2.1129(17) Å is consistent with Fe–$C_{sp^3}$ distances reported for other

TABLE 3. Fractional coordinates of the non-hydrogen atoms and equivalent isotropic thermal parameters for complex **12b**

| Atom | *x* | *y* | *z* | $U_{eq}$, (Å$^2$) [a] |
|---|---|---|---|---|
| Fe | 0.26492(3) | 1.10220(3) | 0.19760(2) | 0.0100(1) |
| O(1) | 0.57929(18) | 0.81767(17) | 0.21570(11) | 0.0259(4) |
| O(2) | 0.42526(17) | 1.32999(16) | 0.12370(9) | 0.0204(4) |
| O(3) | 0.32211(17) | 0.97802(17) | 0.00564(9) | 0.0211(4) |
| O(4) | 0.04828(18) | 1.18499(16) | 0.46975(8) | 0.0179(4) |
| O(5) | −0.15423(18) | 1.43519(18) | 0.48180(9) | 0.0252(4) |
| O(6) | 0.52968(17) | 1.11100(16) | 0.35394(9) | 0.0204(4) |
| O(7) | 0.38663(16) | 1.37716(16) | 0.33516(9) | 0.0178(4) |
| O(8) | 0.03115(17) | 1.30006(16) | 0.03509(8) | 0.0185(4) |
| O(9) | −0.20557(16) | 1.43531(16) | 0.13616(8) | 0.0171(4) |
| N | 0.12030(18) | 0.97873(17) | 0.26383(10) | 0.0114(4) |
| C(1) | 0.4599(2) | 0.9286(2) | 0.21206(12) | 0.0154(5) |
| C(2) | 0.3647(2) | 1.2395(2) | 0.15376(11) | 0.0145(5) |
| C(3) | 0.2872(2) | 1.0275(2) | 0.07987(12) | 0.0152(5) |
| C(4) | 0.0417(2) | 0.8744(2) | 0.22168(12) | 0.0133(4) |
| C(5) | 0.1899(2) | 0.7223(2) | 0.17493(13) | 0.0196(5) |
| C(6) | −0.0651(2) | 0.9747(2) | 0.15273(12) | 0.0168(5) |
| C(7) | −0.0731(2) | 0.8168(2) | 0.29333(13) | 0.0179(5) |
| C(8) | 0.1025(2) | 0.9883(2) | 0.35095(12) | 0.0140(5) |
| C(9) | 0.1862(2) | 1.0798(2) | 0.39778(11) | 0.0137(4) |
| C(10) | 0.3160(3) | 0.9585(2) | 0.44910(13) | 0.0217(6) |
| C(11) | −0.0257(2) | 1.3374(2) | 0.43931(12) | 0.0170(5) |
| C(12) | 0.0773(2) | 1.3591(2) | 0.34975(11) | 0.0127(4) |
| C(13) | 0.2365(2) | 1.1990(2) | 0.33175(11) | 0.0115(4) |
| C(14) | 0.3990(2) | 1.2203(3) | 0.34329(11) | 0.0139(4) |
| C(15) | 0.5389(3) | 1.4079(3) | 0.34348(16) | 0.0269(6) |
| C(16) | −0.0205(2) | 1.3909(2) | 0.27221(11) | 0.0128(4) |
| C(17) | 0.0471(2) | 1.2943(2) | 0.19541(11) | 0.0122(5) |
| C(18) | −0.0387(2) | 1.3407(2) | 0.11371(12) | 0.0131(4) |
| C(19) | −0.2919(2) | 1.4954(3) | 0.05919(13) | 0.0199(5) |

[a] $U_{eq} = 1/3\Sigma\Sigma U_{ij} a_i^* a_j^* \boldsymbol{a}_i \cdot \boldsymbol{a}_j$

complexes (2.07–2.15 Å) [2j,11b,c,12]. The nitrogen containing metallacycle (FeNC(8)C(9)C(13)) in complex **12b** is slightly distorted (±0.17 Å deviation from planarity) whereas the other metallacycle (FeC(13)C(12)C(16)C(17)), connected to the former by the common Fe–C(13) bond, is practically planar (±0.04 Å). The planes through these metallacycles are almost perpendicular (87.49(8)°). The absence of relevant strain in both the spine of the heterocyclic ligand and the coordination geometry of the metal indicates that in the observed conformation, which is mainly determined by the rigid sp$^3$-hybridized C(12) and C(19) atoms, the ligand is particularly well-suited to span three facial coordination sites. Consequently all three coordinated atoms of the ligand are trans to a terminal carbonyl. The relatively short Fe–C(2) bond length of the terminal carbonyl trans to the $\sigma$-donating imine nitrogen reflects the increased $\pi$-back donation in this direction. As a consequence of the C–C coupling of C(12) with the unsubstituted alkyne carbon C(16) of the second MP moiety both the C(12)–C(13) and the C(16)–C(17) bond orders are reduced. The former coordinated C(12)–C(13) double bond of the butenolide heterocycle is reduced to a single bond (1.543(2) Å) while the C(16)–C(17) bond length of 1.341(2) Å in **12b** implies a normal double bond.

### 3.4. *Infrared spectroscopy*

The IR data for complexes **9** and **12** are listed in Table 4. The IR spectra of the Fe(CO)$_3$(butenolide) complexes **9** closely resemble those of the DMADC-derived Fe(CO)$_3$(butenolide) complexes reported earlier [2i]. The terminal CO region of complexes **9** shows three strong bands, one at high frequency and two, only partly resolved, just below 2000 cm$^{-1}$. In the organic carbonyl region two bands of medium intensity are observed; that at higher frequency is assigned to the lactone carbonyl group, because the stretching bands of cyclic carbonyls are generally observed at higher wavenumbers than those of open chain ester carbonyls owing to ring strain [13]. The other band is consequently assigned to the carbonyl of the ester fragment.

The terminal carbonyl region of the tricyclic complexes **12** shows two strong bands, a sharp one at high frequency and a broad one just above 2000 cm$^{-1}$. Relative to those for complexes **9** these bands are shifted to higher wavenumbers, in keeping with a decrease in the metal $\pi$-back donation as a result of the

TABLE 4. IR data and elemental analyses for complexes **9** and **12**

| | IR [a,b] $\nu$(CO), cm$^{-1}$ | Elemental analyses | | |
|---|---|---|---|---|
| | | C obs (calc) | H obs (calc) | N obs (calc) |
| **9a** | 2056 (s), 1994 (sh), 1978 (s)<br>1750 (m), 1710 (m) | 54.65 (54.44) | 4.42 (4.34) | 3.22 (3.17) |
| **9b** | 2050 (s), 1985 (sh), 1970 (s)<br>1755 (m), 1705 (m) | 47.00 (47.52) | 4.63 (4.52) | 3.66 (3.69) |
| **12a** | 2071 (s), 2010 (s), 1780 (m),<br>1697 (m) | 54.66 (54.88) | 4.46 (4.42) | 2.74 (2.67) |
| **12b** | 2071 (s), 2011 (s), 1776 (m),<br>1695 (m) | 49.06 (49.26) | 4.80 (4.57) | 3.04 (3.02) |

[a] s = strong, sh = shoulder, m = medium. [b] Measured in THF.

change of the formal oxidation state of the central iron atom from Fe(0) to Fe(II). Although there are three organic ketone fragments present in complexes **12** only two bands of medium intensity are observed in the $\nu$(C=O) region. The high frequency band (1780 $cm^{-1}$) is again assigned to the cyclic ester carbonyl. The absorptions of the two ester carbonyl groups probably coincide by chance, giving rise to a single band at 1700 $cm^{-1}$.

### *3.5. NMR spectroscopy*

#### *3.5.1. Complexes 9*

The $^1H$ and $^{13}C$ NMR data for **9a**, **b** are listed in Tables 5 and 6 respectively, with the atom numbering given in Fig. 1. The $^1H$ and $^{13}C$ NMR spectra of complexes **9** closely resemble those of the DMADC-derived $Fe(CO)_3$(butenolide) complexes reported earlier [2i], and since the NMR data for the latter complexes have already been extensively discussed, we focus below mainly on some anomalous features and the spectroscopic characterization of the regio-isomer obtained.

The resonances of the methoxy protons (H(15)) in **9a** ($\delta = 3.32$ ppm) are shifted upfield relative to those from complex **9b** ($\delta = 3.68$ ppm); this is probably due to the proximity of the ester group to the anisotropic phenyl substituent at the bridgehead carbon atom. The phenyl protons in **9a** give rise to one single resonance, indicating that they are by chance magnetically equivalent. The alkene proton resonances (H(12), *vide infra*) in complexes **9a, b**, observed as singlets at 4.18 and 4.06 ppm, respectively, are within the range normally found for protons on a coordinated double bond. It should be noted that the observed intensities of these resonances are too low as a result of partial saturation due to the very long spin-spin relaxation time of the protons ($T_1 \approx 17$ s), and this in turn is likely to be due to their isolated position.

TABLE 6. $^{13}C$ NMR Data for complexes **9** and **12**

| | δ-values [a] | | | |
|---|---|---|---|---|
| | **9a** [a] | **9b** [a] | **12a** | **12b** |
| Nucleus | | | | |
| C(1), (2), (3) | 210.1 | 210.0 | 209.4 | 209.1 |
| | 209.3 | 209.5 | 205.4 | 205.4 |
| | 207.9 | 208.1 | 203.7 | 204.0 |
| C(4) | 65.9 | 65.3 | 66.2 | 65.5 |
| C(5), (6), (7) | 31.0 | 30.8 | 30.1 | 30.8 |
| C(8) | 176.9 | 177.7 | 173.0 | 175.9 |
| C(9) | 92.8 | 90.2 | 100.2 | 97.6 |
| C(10) | 134.8 | 19.8 | 135.7 | 21.4 |
| C(11) [b] | 174.8 | 174.7 | 177.1 | 177.0 |
| C(12) | 45.7 | 46.8 | 60.7 | 60.4 |
| C(13) | 74.6 | 71.7 | 68.4 | 63.5 |
| C(14) [b] | 172.2 | 172.1 | 175.6 | 175.1 |
| C(15) [c] | 51.4 | 51.7 | 52.4 | 52.4 |
| C(16) | – | – | 151.6 | 151.8 |
| C(17) | – | – | 160.4 | 161.1 |
| C(18) [b] | – | – | 173.0 | 172.9 |
| C(19) [c] | – | – | 52.2 | 52.4 |
| C(20), (21), (22) | 128.6 | – | 129.1 | – |
| | 126.3 | – | 125.3 | – |
| | 129.6 | – | 129.6 | – |

[a] δ-values (in ppm, relative to TMS) have been measured in $CDCl_3$ solution at 263 K and 25.15 MHz. [b,c] Individualised assignments are tentative.

Because in the IR, $^1H$, and $^{13}C$ NMR spectra only one of the two possible regio-isomers of complexes **9** were observed, INEPT and heteronuclear *J*-correlated 2D NMR techniques were used to decide between the two regio-isomers of **9b** (see Fig. 1). In the INEPT spectrum, which was optimized for a $J(^1H-^{13}C)$ between 3 and 7 Hz, a coupling constant of 3.9 Hz was found for the carbonyl carbon atom C(11) while for the bridgehead carbon atom C(9) several coupling constants were observed. The magnitude of the coupling constant at C(11) suggests that we are dealing with regio-isomer A, but it does not fully exclude isomer B because it could also be the result of a large $^3J(^1H-^{13}C)$

TABLE 5. $^1H$ NMR data for complexes **9** and **12**

| | δ-values (ppm, multiplicity, coupling constant, rel. intensity [a,b] | | | |
|---|---|---|---|---|
| | **9a** | **9b** | **12a** | **12b** |
| Nucleus | | | | |
| H(5), (6), (7) | 1.38, s, 9H | 1.32, s, 9H | 1.45, s, 9H | 1.30, s, 9H |
| H(8) | 8.10, s, 1H | 7.67, s, 1H | 7.70, s, 1H | 7.51, s, 1H |
| H(10) | – | 1.87, s, 3H | – | 1.70, s, 3H |
| H(12) | 4.18, s, 1H | 4.06, s, 1H | 5.05, d, 3.3, 1H | 4.9, d, 3.4, 1H |
| H(15) | 3.32, s, 3H | 3.68, s, 3H | 3.15, s, 3H | 3.71, s, 3H |
| H(16) | – | – | 7.11, d, 3.3, 1H | 7.06, d, 3.4, 1H |
| H(19) | – | – | 3.73, s, 3H | 3.75, s, 3H |
| H(20), (21), (22) | 7.42, s, 5H | – | 7.17–7.44, m, 5H | – |

[a] δ-values (in ppm, relative to TMS) have been measured in $CDCl_3$ solution at 293 K and 100.1 MHz. [b] s = singlet, d = doublet, m = multiplet.

coupling. In the latter case an additional $^{2}J(^{1}H-^{13}C)$ of the alkene proton with C(9) of *ca.* 4–7 Hz would be expected, which could not be deduced directly from the INEPT spectra. We therefore recorded the heteronuclear correlated 2D spectra ($J(^{1}H-^{13}C) = 4$ and 6 Hz), which show that there is no correlation of the alkene proton with C(9). The proton in question does correlate with C(11), which confirms that regio-isomer A is exclusively obtained. From the corresponding $^{13}C$ NMR data a similar structure is assigned to complex **9a**.

### 3.5.2. Complexes 12

The $^{1}H$ and $^{13}C$ NMR data for **12a**, **b** are listed in Tables 5 and 6 respectively, and the atom numbering is given in Fig. 2. The NMR data of complexes **12** in solution are consistent with the structure in the solid state. The imine proton resonances H(8) of complexes **12** are shifted slightly upfield relative to those for complexes **9**. The resonances of the former MP protons H(12) and H(16) are observed as doublets at *ca.* 5.0 and 7.1 ppm, respectively. The relatively small coupling constant between H(12) and H(16) ($^{3}J = 3.3$ Hz) points to a large dihedral angle of the C–H bonds in question (*ca.* 70° in the solid state). As in the butenolide complex **9a**, the resonance of one of the ester methyl groups (H(15)) of **12a** is shifted upfield ($\delta = 3.15$ ppm).

The terminal carbonyl ligands of complexes **12** resonate at between 203 and 209 ppm, which is slightly upfield relative to those for complexes **9** reflecting the small decrease in $\pi$ back-donation (also observed in the IR spectrum). Apart from those of the carbon atoms directly involved in the C–C coupling reaction, the $^{13}C$ resonances of the heterocyclic ligand in **12** are observed at positions similar to those for the $Fe(CO)_3$(butenolide) complexes. The resonances of the $sp^2$-metallated C(17) (ca. 160 ppm) are shifted upfield relative to those observed for similar $\sigma$-coordinated carbon atoms in the ferrabicyclo[2.2.2] complexes **3** ($\Delta\delta \approx 30$ ppm) [2b], but agree well with those reported by tom Dieck *et al.* for this type of carbon atom in ferracyclopentadiene complexes [9b]. The fact that the $sp^3$ carbon atom C(12) is adjacent to both a carbonyl and an alkene moiety probably accounts for its relatively high $\delta$ value (66 ppm).

### 3.6. Complex formation

The formation of complexes **9** and **12** can be readily explained in terms of the mechanism depicted in Scheme 2. It should be noted that the intermediates in this sequence could not be isolated nor detected [14*] and their intermedicacy is based on the analogy with the reactions of the related $M(CO)_3$(R-DAB) (M = Fe, Ru) complexes with activated alkynes. In considering the detail of the intimate steps in this mechanism, especially the initial reaction, it is thus necessary to summarize some results described in earlier parts of this series. Therein we demonstrated that the Fe–N=C and the Fe–O=C fragments are isolobally related to an azomethine and a carbonyl ylide, respectively, two well-known classical organic 1,3-dipoles. On the basis of comparison with the organic ylides and on theoretical CAS-CSF calculations on the model systems $Fe(CO)_3(NH{=}C(H){-}C(H){=}X)$ (X = N–R, O) [2i], the organometallic 1,3-dipoles can be classified as nucleophilic or type I 1,3-dipoles [15*]; i.e., they possess relatively high lying frontier orbitals and react preferentially with electron deficient dipolarophiles. Cycloaddition reactions of this type of 1,3-dipole are HOMO-controlled (the interaction of the dipole HOMO with the dipolarphile LUMO is dominant). Furthermore, it has been shown that when both the Fe–N=C and the Fe–O=C fragment are present in one molecule, the activated alkyne exclusively reacts with the Fe–O=C dipole, indicating that the latter fragment is for both electronic and steric reasons, the more reactive.

The initial step in the proposed mechanism is thus an oxidative 1,3-dipolar cycloaddition reaction of MP to the Fe–O=C fragment, to give the bicyclo[2.2.1] intermediate **7**. Since the organometallic dipole is isolobally related to a carbonyl ylide, the explanation of the observed reactivity and regioselectivity in this initial reaction will be largely based on the theoretical concept for the organic 1,3-dipolar cycloadditions, developed by Houk *et al.* [16]. We are aware that the shape and size of the metal d-orbitals may also exert a considerable influence, but there is insufficient relevant information to justify definite conclusions or to indicate general trends with respect to their contribution. Qualitatively, the preferred regio-isomer in a 1,3-dipolar cycloaddition will be that one in which the atoms with the larger terminal coefficients of the interacting frontier orbitals interact. Control of regioselectivity by the dipole HOMO will lead to products with the substituent remote from the 'anionic' terminus for electron deficient dipolarophiles (larger coefficient at the unsubstituted carbon atom in the LUMO) [16]. Because the organometallic cycloaddition has been shown to be HOMO-controlled and the larger coefficient of the HOMO probably resides on the iron atom, namely the 'anionic' terminus (which is confirmed by the CAS-SCF calculations), the experimentally observed regioselectivity is to a large extent rationalized. Steric hindrance to the approach of the alkyne probably plays a subordinate role, since complexes **6** also react readily with DMADC. The somewhat slower reaction observed for the phenyl-substituted complex **6a** is in agreement with the theoretical finding that in

HOMO-controlled cycloaddition reactions the presence of electron-withdrawing substituents in the 1,3-dipole lowers the reaction rate.

The initial step is followed by an insertion of a terminal CO ligand into the Fe–O bond, giving rise to a coordinatively unsaturated species, and at that stage the reaction can take one of two courses, depending on the nature of the additional ligand offered. If CO is offered, the reaction proceeds via the 'normal' route, *i.e.* formation of the coordinatively saturated bicyclo [2.2.2] intermediate **8** which then rapidly isomerizes (reductive elimination of the two covalently bound carbon atoms followed by recoordination of the double bond) to form the Fe(CO)$_3$(butenolide) complex **9**. When an excess of MP is present as additional ligand, the bicyclo[2.2.2] intermediate **10** is formed, which in turn readily isomerizes to give the butenolide intermediate **11**. The finding that complexes **12** can also be readily obtained by irradiation of complexes **9** in the presence of an excess of MP supports the suggestion that the $\gamma$-lactone ring is formed by reductive elimination prior to the C–C coupling. Intermediate **11** subsequently undergoes a C–C coupling between the unsubstituted carbon atom of the $\pi$-coordinated MP moiety and the unsubstituted carbon atom of the $\pi$-coordinated C=C bond of the butenolide heterocycle, which results in formation of the final product **12**. In this process two covalent Fe–C bonds are formed and the central iron atom changes in oxidation state from Fe(0) to Fe(II). A substantial number of comparable C–C coupling reactions involving two $\pi$-coordinated alkenes [11,17] or alkynes [9] are encountered in the formation of five-membered metallacycles, but coupling of an alkene with an alkyne is less common.

Stockis and Hoffmann have demonstrated that the regioselectivity in these C–C coupling reactions results from a combination of electronic and steric effects [17]. On the basis of consideration of perturbation effects on the frontier orbitals in the bisethylene/metallacyclopentane interconversion (on the iron tricarbonyl system) and a polarization model for asymmetrical alkenes [18] they developed a generalized theoretical concept, that in a number of cases successfully predicts experimentally observed selectivities. The orbital strongly involved in the formation of the new C–C bond is mainly localized on the ligand and is dominated by $\pi^*$-contribution (the interaction of the relevant $\pi$-orbitals is repulsive). Therefore the preferred linkage-isomer will be the one that has the largest lobes for the $\pi^*$-orbitals of both components in a $\beta$-position to the metal. Since the larger coefficients in the $\pi^*$-orbitals of both mono-substituted electron deficient alkenes and alkynes have been shown to reside on the unsubstituted carbon atom [16,18], the experimentally observed regioselectivity in the formation of complexes **12** is in agreement with the theoretical model. Comparable regioselectivity is observed in the C–C coupling reactions following the irradiation of Fe(CO)$_4$($\eta^2$-methyl acrylate) in the presence of an excess of methyl acrylate or a butadiene [11].

## Acknowledgements

The investigation was supported in part (A.L. Spek) by the Netherlands Foundation for Chemical Research (SON) with financial aid from the Netherlands Organization for Scientific Research (NWO). The X-ray data for **12b** were kindly collected by A.J.M. Duisenberg.

## References and notes

1 The abbreviations used throughout this text are as follows. The 1,4-diaza-1,3-butadienes of formula RN=C(H)C(H)=NR are abbreviated as R-DAB. THPP stands for 1,4,3a,6a-tetrahydropyrrolo[3,2-*b*] pyrrole (Hantzsch-Widman nomenclature). Dimethyl acetylenedicarboxylate and methyl propynoate are abbreviated as DMADC and MP respectively.

2 (a) Part 1: H.-W. Frühauf, F. Seils, M.J. Romão and R.J. Goddard, *Angew. Chem.*, *95* (1983) 1014; (b) Part 2: H.-W. Frühauf, F. Seils, R.J. Goddard and M.J. Romão, *Organometallics*, *4* (1985) 948; (c) Part 3: H.-W. Frühauf and F. Seils, *J. Organomet. Chem.*, *302* (1986) 59; (d) Part 4: H.-W. Frühauf and F. Seils, *J. Organomet. Chem.*, 323 (1987) 67; (e) Part 5: H.-W. Frühauf, F. Seils and C.H. Stam, *Organometallics*, *8* (1989) 2338; (f) Part 6: P.P.M. de Lange, H.-W. Frühauf, M. van Wijnkoop, K. Vrieze, Y. Wang, D. Heijdenrijk and C.H. Stam, *Organometallics*, *9* (1990) 1691; (g) Part 7: M. van Wijnkoop, P.P.M. de Lange, H.-W. Frühauf, Y. Wang, K. Goubitz and C.H. Stam, *Organometallics*, *11* (1992) 3607; (h) Part 8: P.P.M. de Lange, H.-W. Frühauf, M. van Wijnkoop, M.J.A. Kraakman, M. Kranenburg, A.H.J.P. Groot, K. Vrieze, J. Fraanje, Y. Wang and M. Numan, *Organometallics*, *12* (1993) 417; (i) Part 9: M. Van Wijnkoop, R. Siebenlist, P.P.M. de Lange, H.-W. Frühauf, K. Vrieze, W.J.J. Smeets and A.L. Spek, *Organometallics*, *12* (1993) 4172; (j) Part 10: P.P.M. de Lange, M. van Wijnkoop, H.-W. Frühauf, K. Vrieze, and K. Goubitz, *Organometallics*, *12* (1993) 428; (h) Part 11: P.P.M. de Lange, R.P. de Boer, M. van Wijnkoop, J.M. Ernsting, H.-W. Frühauf, K. Vrieze, W.J.J. Smeets, A.L. Spek and K. Goubitz, *Organometallics*, *12* (1993) 440; (i) Part 12: P.P.M. de Lange, E. Alberts, M. van Wijnkoop, H.-W. Frühauf, K. Vrieze, H. Kooijman and A.L. Spek, *J. Organomet. Chem.*, *465* (1994) 241.

3 (a) H. van der Poel and G. van Koten, *Synth. Comm.*, *8* (1978) 305; (b) B. Alcaide, G. Escobar, R. Pérez-Ossario, J. Plumet and D. Sanz, *J. Chem. Research* (M), (1984) 1466, see also *J. Chem. Research* (S), (1984) 144.

4 G.M. Sheldrick, SHELXS86 *Program for Crystal Structure Determination*, Univ. of Göttingen, Germany, 1986.

5 G.M. Sheldrick, SHELX76, *Crystal Structure Analysis Package*, Cambridge University, 1976.

6 D.T. Cromer, and J.B. Mann, *Acta Crystallogr.*, *A24* (1968) 321.

7 D.T. Cromer, and D. Liberman, *J. Chem. Phys.*, *53* (1970) 1891.

8 A.L. Spek, *Acta Crystallogr.*, *A46* (1990) C34.

9 (a) E. Lindner, R.-M. Jansen, H.A. Mayer, W. Hiller and R. Fawzi, *Organometallics*, *8* (1989) 2355; (b) H. tom Dieck, R.

Diercks, L. Stamp, H. Burder and T. Schuld, *Chem. Ber.*, *120* (1987) 1943.

10 (a) L.F. Dahl, R.J. Doedens, W. Hübel and J. Nielsen, *J. Am. Chem. Soc.*, *88* (1966) 446; (b) R. Birk, U. Grössman, H.-U. Hund and H. Berke, *J. Organomet. Chem.*, *345* (1988) 321; (c) E. Lindner, C.P. Krieg, W. Hiller and R. Fawzi, *Angew. Chem.*, *96* (1984) 508; (d) F. Muller, G. van Koten, K. Vrieze and D. Heijdenrijk, *Inorg. Chim. Acta*, *158* (1989) 69.

11 (a) F.-W. Grevels, D. Schulz and E. Koerner v. Gustorf, *Angew. Chem.*, *86* (1974) 558; (b) C. Krüger and Y.-H. Tsay, *Cryst. Struct. Comm.*, *5* (1976) 215; (c) F.-W. Grevels, U. Feldhoff, J. Leitich and C. Krüger, *J. Organomet. Chem.*, *118* (1976) 79.

12 (a) E. Lindner, E. Schauss, W. Hiller and R. Fawzi, *Angew. Chem.*, *96* (1984) 727; (b) P. Eilbracht, R. Jelitte and L. Walz, *Chem. Ber.*, *117* (1984) 3473; (c) H. Kisch, C. Krüger, H.E. Marcolin and A.X. Trautwein, *Z. Naturforsch. Teil B.*, *42* (1987) 1435.

13 M. Hesse, H. Meier and B. Zeeh, in *Spektroskopische Methoden in der Organischen Chemie*, Georg Thieme Verlag, Stuttgart, New York, 1984.

14 A bicyclo[2.2.2] complex, analogous to intermediate **8**, formed in the reaction of $Fe(CO)_3(Me-N=C(Ph)-C(Ph)=O)$ with DMADC has recently been spectroscopically characterized at low temperature (R. Siebenlist, unpublished results).

15 Application of the Frontier Molecular Orbital Theory to 1,3-dipolar cycloadditions by Sustmann provides a semi quantitative classification of these cycloadditions into three types depending on the relative disposition of the 1,3-dipole and the dipolarophile frontier orbitals. (a) R. Sustmann, *Tetrahedron Lett.*, (1971) 2717; (b) R. Sustmann, and H. Trill, *Angew. Chem., Int. Ed. Engl.*, *11* (1972) 838; (c) R. Sustmann, *Pure Appl. Chem.*, *40* (1974) 569.

16 (a) K.N. Houk, J. Sims, R.E. Duke Jr., R.W. Stozier and J.K. George, *J. Am. Chem. Soc.*, *95* (1973) 7287; (b) K.N. Houk, J. Sims, C.R. Watts and L.J. Luskus, *J. Am. Chem. Soc.*, *95* (1973) 7301.

17 A. Stockis, and R. Hoffmann, *J. Am. Chem. Soc.*, *102* (1980) 2952 and references cited therein.

18 L. Libit, and R. Hoffmann, *J. Am. Chem. Soc.*, *96* (1974) 1370.